https://doi.org/10.5194/egusphere-2025-4005
Preprint. Discussion started: 9 September 2025

Elevated Anthropogenic Contributions to Trace Elements in Marine Aerosols Compared to Coastal Qingdao in Eastern China

Yuxuan Qi[1,2], Wenshuai Li[1,2,3,4], Wen Qu[5], Haizhou Zhang[5], Wenqing Zhu[1,2], Jinhui Shi[3,4], Daizhou Zhang[6], Yanjing Zhang[1,2], Lifang Sheng[1,2], Wencai Wang[1,2], Yunhui Zhao[1,2], Yuanyuan Ma[1,2], Danyang Ren[1,2], Guanru Wu[1,2], Xinfeng Wang[7], Xiaohong Yao[3,4], Yang Zhou[1,2*]

[1]State Key Laboratory of Physical Oceanography, Ocean University of China, Qingdao, 266100, China
[2]College of Oceanic and Atmospheric Sciences, Ocean University of China, Qingdao, 266100, China
[3]Key Laboratory of Marine Environment and Ecology, Ministry of Education, Ocean University of China, Qingdao, 266100, China
[4]Laboratory for Marine Ecology and Environmental Science, Qingdao National Laboratory for Marine Science and Technology, Qingdao, 266237, China
[5]North Sea Bureau of Ministry of Natural Resources of the People's Republic of China, Qingdao, 266061, China
[6]Faculty of Environmental and Symbiotic Sciences, Prefectural University of Kumamoto, 862-8502, Japan
[7]Environment Research Institute, Shandong University, Qingdao, 266237, China

Correspondence to: Yang Zhou (yangzhou@ouc.edu.cn)

Abstract. Trace elements (TEs) in aerosols over offshore eastern China originate from both terrestrial and marine emissions. However, their variations with source regions remain poorly understood. During spring and summer 2018, $PM_{2.5}$ samples were collected at Qingdao, a coastal city in eastern China, and adjacent Bohai and Yellow Seas. TEs were quantified and analyzed by source region, followed by source apportionment. In spring, TE concentrations were significantly higher over land. Crustal dust contributed 39.2–77.8% of Fe, Mn, Cr and Ni; while waste and industrial emissions contributed 29.4–70.1% of Cu, Zn and Pb. Westerly winds conveyed anthropogenic TEs offshore, with coal combustion contributing 25.9–61.4% to As, Cd, Pb, Zn and Cr, and oil combustion contributing 58.6–84.4% to V and Ni in marine aerosols, indicating efficient long-range pollutant transport. In summer, dust influence declined. Biomass burning contributed 38.2–46.3% of Zn, Cd, Pb and Cr, while vehicular emissions dominated As and Cu (41.7–57.3%) at Qingdao. Over marine areas, anthropogenic elements (Zn, As, and Cd) occasionally exceeded coastal levels, with coal combustion remaining dominant (40.8–75.5%). Ship emissions became especially prominent, contributing 79.3% of V and 63.3% of Ni offshore. Southeasterly winds transported ship-derived pollutants coastward, markedly increasing Fe (21.2%) and Mn (14.0%) compared to spring (1.9% and 1.8%, respectively). These results reveal distinct seasonal shifts in TE source across land-sea gradients, highlighting growing anthropogenic impacts, particularly from coal combustion and maritime shipping on marine aerosols. Quantifying these contributions helps assess marine biogeochemical impacts and supports targeted pollution control.

https://doi.org/10.5194/egusphere-2025-4005
Preprint. Discussion started: 9 September 2025

1 Introduction

Atmospheric aerosols can significantly impact the local environment and global climate change through modifying the solar radiation balance in the atmosphere (Huang et al., 2014; Ramanathan et al., 2007) and supplying nutrients to ecosystems (Choobari et al., 2014). Anthropogenic activities release a profusion of pollutants that can engage in intricate physicochemical processes, resulting in the formation of atmospheric fine particulate matter ($D_p \leq 2.5$ μm, $PM_{2.5}$). Distinct from large-diameter particles, these primary or secondary $PM_{2.5}$ usually possess long lifetimes, which are capable of undergoing long-range transport in the atmosphere and depositing into remote oceans. This process introduces substantial anthropogenic pollutants, thereby impacting ocean ecosystems (Mahowald, 2011; Xu et al., 2021).

Despite trace elements constituting only a minor fraction of the $PM_{2.5}$ mass, their significant post-deposition impacts on downwind marine ecosystems have attracted considerable attention (Li et al., 2015; Morel and Price, 2003; Zhang et al., 2018). Some trace elements deposited in the open oceans, such as Mn, Fe, Ni, Cu, Zn, and Cd, have biological roles, generally as cofactors or part of cofactors of enzymes or as structural elements in proteins (Morel and Price, 2003). These elements can markedly influence the growth of phytoplankton taxa and the biological community structure of marine organisms, thereby affecting carbon sequestration and marine primary production (Boyd et al., 2000; Falkowski et al., 1998; Mann et al., 2002; Martin, 1990; Morel and Price, 2003; Yoon et al., 2018; Tang et al., 2021). The total fraction of trace elements cannot be fully utilized. In most cases, only the soluble fractions of elements are more likely to be bioavailable (Shi et al., 2012). The soluble fractions (i.e., solubility) of elements are closely associated with their sources (Baker et al., 2006; Sholkovitz et al., 2012). For instance, while mineral dust is the principal source of Fe, numerous studies have demonstrated that Fe emitted from anthropogenic sources has a higher solubility (López-García et al., 2017; Sholkovitz et al., 2012; Sun et al., 2024). Model results also suggest that the combustion-derived Fe tended to account for over 20% of the Fe deposition near the Asian continent, and the efficiency of pyrogenic Fe in enhancing marine productivity exceeds that of lithogenic sources (Ito et al., 2021; Luo et al., 2008). Fe from the combustion source is typically present in finer particles (Buck et al., 2010; Ito and Feng, 2011). Therefore, it is essential to evaluate both the nature and anthropogenic sources of $PM_{2.5}$ as well as these trace elements over marine regions.

The Bohai Sea (BS) and Yellow Sea (YS) are on the crucial transport pathway for aerosols originating from the heavily polluted East Asia area to the Northwest Pacific within the westerly belt. Qingdao (QD) is a coastal city adjacent to YS (Fig.1). Aerosol trace elements over the BS and YS likely exhibit distinct characteristics compared to those in coastal cities, necessitating synchronized land-sea observations to investigate these characteristics. However, as previously noted, the current knowledge regarding the source apportionment of trace elements in marine aerosols remains limited (Hilario et al., 2020). Prior field cruise investigations have focused on studying the particle characteristics of total suspended particulates (TSP) and PM_{10} ($D_p \leq 10$ μm) (Hsu et al., 2010; Li et al., 2025; Peng et al., 2025; Qiu, 2015; Shi et al., 2013; Wang et al., 2013; Yang et al., 2020). In contrast, trace elements in $PM_{2.5}$ have been scarcely explored. Previous research at Qingdao revealed that the soluble Fe

https://doi.org/10.5194/egusphere-2025-4005
Preprint. Discussion started: 9 September 2025

concentration in fine particles is three-fold higher than that in coarse mode (Li et al., 2018). Moreover, the solubility of Fe was notably greater in fine particles compared to coarse particles (Zhang et al., 2022).

Atmospheric processes that occurs during long-range transport from the continent to ocean can significantly enhance the solubility of trace elements and influence the ecosystems of the surface ocean by dry and wet deposition (Schroth et al., 2009; Sholkovitz et al., 2012; Wang et al., 2022; Wang et al., 2021; Luo et al., 2020; Xu et al., 2023; Zhang et al., 2024). Understanding how and to what degree these processes alter the sources of trace elements during transport is crucial for assessing the impact of anthropogenic pollution on the marine ecosystem. This study conducted simultaneous observations in Qingdao and during BS and YS research cruises in the spring and summer of 2018 (Fig.1), investigating the characteristics and source apportionment of trace elements. This work contributes to a more comprehensive understanding of the distribution and sources of trace elements in fine particles from coastal to marginal sea areas in eastern China and complicated spread of aerosols.

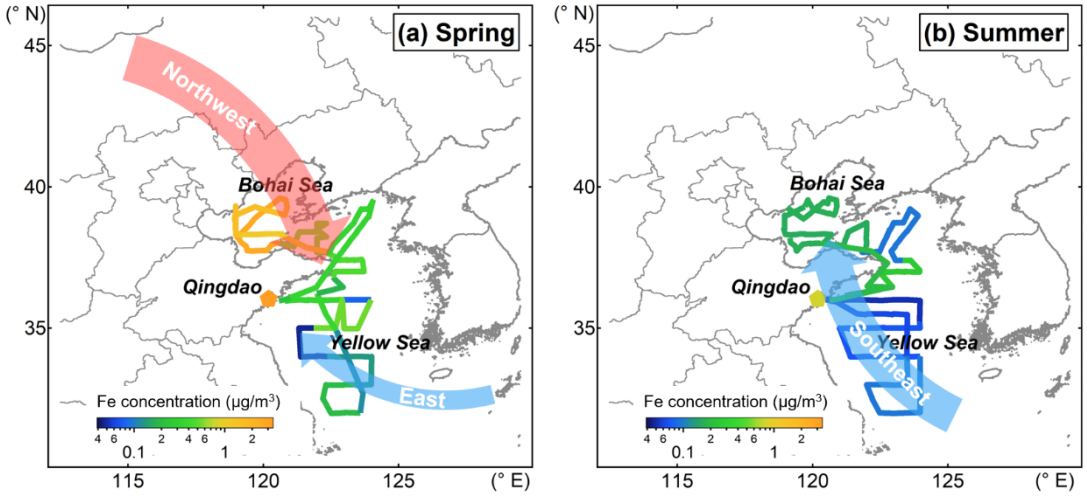

Figure 1: Schematic diagram of regional maps with dominant air mass transport pathways (arrows). The solid lines indicate cruise tracks for (a) springtime and (b) summertime cruises over BS and YS during 2018 and the star indicates the location of Qingdao, with the color-filled indicating Fe concentration.

2 Methodology

2.1 Sample collection

$PM_{2.5}$ samples were collected to measure fine particle components over the BS, YS, and Qingdao during the spring and summer of 2018. In the cruise missions, the samples were collected over the BS and YS from 28 March to 17 April and from 24 July to 10 August 2018. These areas are located in the downwind areas of the Asian dust source regions and northern China city groups being significantly influenced by dust and anthropogenic pollution (Fig.1). Eighteen and nine samples were collected

https://doi.org/10.5194/egusphere-2025-4005
Preprint. Discussion started: 9 September 2025

during non-rainy periods in spring and summer, respectively. During the collection of marine aerosols, samples were exclusively collected while the ship was underway to avoid contamination from the exhaust emissions.

The samples in Qingdao were collected in the same period as the cruise missions. The sampling site was located at the Baguanshan Atmospheric Research Observatory (BARO, 36.03° N, 120.20° E; 74 m above sea level) in the Shinan District Qingdao (Fig.1), with a approximately 600 m straight-line distance from the coastline (Li et al., 2024; Yang et al., 2024). Thirty-seven and twenty-five samples were collected during non-rainy periods in spring and summer, respectively.

High-volume particle samplers (Tisch Environmental, Inc., USA and Qingdao Jinshida Electronic Technology Co., Ltd., China) were applied to collect the particles onto Whatman® 41# filters (Whatman Limited, Maidstone, UK) for trace element analysis, and onto PALL® quartz filters (Pall Gelman, Inc., USA) for analysis of water-soluble ions, organic carbon (OC), and elemental carbon (EC). The 41# filters were washed with diluted acid prior to sampling following Chance et al. (2015) to remove background trace elements. Quartz filters were pre-baked at 450 °C for 6 hours before the sample collection to eliminate background organic contaminants. Blank filters were collected for quality assurance and control. All samples were sealed in plastic bags and stored at -20 °C until subsequent analysis.

2.2 Chemical analysis

Trace elements: An 8.0 cm^2 section of both the sample and blank filters was digested with an acid mixture (2.0 mL of 69% HNO_3 and 0.5 mL of 40% HF) in closed Teflon vessels and heated at 180 °C for 48 h. After cooling to room temperature, the solutions were evaporated to near dryness at 180 °C using an electric heating plate. Then, the residue was diluted to 50 mL with 2% HNO_3 and stored at ~4 °C until analysis.

The concentrations of elements in the extracts were measured using an inductively coupled plasma-mass spectrometry (ICP-MS, iCAP Qc, Thermo Fisher Scientific, Germany) with internal standards of Rh, Sc, and Th to eliminate matrix interference. A standard solution was analyzed as a quality control sample for every 10 samples.

Water-soluble ions: Sample sections and blank filters were extracted with 10 mL Milli-Q water (≥18.0 MΩ·cm) using ultrasonication for 40 min at 0 °C followed by filtration through a 0.45 μm pore diameter filter, then stored at ~4 °C until analysis in 3 days. Water-soluble ionic species, including Na^+, NH_4^+, K^+, Mg^{2+}, Ca^{2+}, Cl^-, NO_3^-, SO_4^{2-} and $C_2O_4^{2-}$, were analyzed using a Dionex ICS-3000 ion chromatography. Blank filter solution and standard solution were analyzed for every 10 samples to control the quality.

OC and EC: 2.0 cm^2 section of samples and blank filters were analyzed by Sunset OC/EC analyzer using NIOSH protocol (Wu et al., 2016). The data obtained were calibrated with a standard curve.

2.3 Other data and backward trajectories

Meteorological parameters during the sample collection periods, including relative humidity (RH), wind speed (WS) and wind direction, were obtained from the shipboard measurements and Qingdao Meteorological Bureau, and monitoring data of

https://doi.org/10.5194/egusphere-2025-4005
Preprint. Discussion started: 9 September 2025

gaseous pollutants, including SO_2, NO_2, O_3, and CO, were from China National Environmental Monitoring Centre (http://www.cnemc.cn/, https://quotsoft.net/air/).

The Hybrid Single-Particle Lagrangian Integrated Trajectory (HYSPLIT) model (PC v4.8) developed by the National Oceanic and Atmospheric Administration Air Resources Laboratory (NOAA-ARL) (Draxler and Rolph, 2014) was employed to reconstruct the three-dimensional 72-h backward trajectories. This was done to identify distinct air mass source regions and their transport paths. The starting point for the trajectory calculations was set at an altitude of 300 m above the ground level. The calculations were performed with the vertical velocity calculation method and archived Global Data Assimilation System (GDAS) meteorological data.

2.4 Positive matrix factorization receptor model

The Positive Matrix Factorization (PMF) model is a widely used receptor model to resolve pollution sources and quantify the source contributions to ambient particulate matter concentrations (Paatero and Tapper, 1994). It decomposes the measured data matrix into factor profile, contribution, and residual matrix. In this study, the Environmental Protection Agency (EPA) PMF version 5.0 was utilized for analysis (Norris et al., 2014).

In this study, the mass concentrations of 13 elements (Al, V, Cr, Mn, Fe, Ni, Co, Cu, Zn, As, Cd, Ba and Pb), 9 water-soluble ions (Na^+, NH_4^+, K^+, Mg^{2+}, Ca^{2+}, Cl^-, NO_3^-, SO_4^{2-} and $C_2O_4^{2-}$), and OC/EC from both coastal and cruise campaigns (81 samples) were input to the PMF analysis. Multiple factors ranging from 6 to 10 were thoroughly evaluated to determine the optimal solution. The stability and reliability of the factor solutions were assessed using the displacement (DISP) and bootstrap (BS) uncertainty estimation methods (Norris et al., 2014). Ultimately, an 8-factor solution emerged as the most robust and interpretable. In contrast, the 7-factor solution failed to distinguish the industrial emissions from dust (Fig.S1a), while the 9-factor solution tended to resolve an additional factor with an extremely low BS mapping value of 58% (Fig.S1b and Table S1). The 8-factor solution demonstrated the highest stability. The mapping percentages using the BS uncertainty method exceeded 75% for all factors (Table S2), surpassing the performances of the 7-factor and 9-factor solutions (Table S3 and S1). Moreover, the DISP analysis showed no occurrences of factor swapping and no reduction in the model fit statistic Q (both %dQ and the error code were 0), further validating the stability and interpretation of the 8-factor solution.

3 Spatiotemporal distributions of trace elements

Figure 2, Tables S4 and S5 summarize the overall average concentrations of elements. Over the BS and YS, the predominant trace elements were Al, Fe, and Zn, with concentrations (average ± standard deviation) of 1043.2 ± 1031.0 ng m^{-3}, 648.6 ± 654.8 ng m^{-3}, and 49.9 ± 75.0 ng m^{-3} in spring, and 93.2 ± 81.8 ng m^{-3}, 122.0 ± 65.7 ng m^{-3}, and 76.6 ± 117.6 ng m^{-3} in summer, followed by Mn (spring) and V (summer) respectively. In the coastal city, the dominant trace elements were Al and Fe, with average concentrations of 5573.5 ± 5641.1 and 3347.3 ± 3249.3 ng m^{-3} in spring and 493.8 ± 395.4 and 228.3 ± 211.7 ng m^{-3} in summer, followed by Mn in spring and Zn in summer, respectively (Fig.2c). Zn was the most abundant anthropogenic

https://doi.org/10.5194/egusphere-2025-4005
Preprint. Discussion started: 9 September 2025

element in both marine and coastal environments. Except for V, element concentrations during summer in Qingdao were lower than those reported by Li et al. (2018) during summer 2016. In this study, V and Ni, as representative tracers of emissions from heavy oil combustion, indicated a higher influence from ship emissions during the campaigns (Li et al., 2020; Zhang et al., 2019b; Zhao et al., 2013).

All elements displayed notably higher concentrations in Qingdao compared to the marine area in spring. However, the discrepancy in concentrations of V, As, and Cd between land and sea was relatively smaller than those of other elements (Fig.2). The region with the lowest recorded concentrations was observed over YS in both spring and summer. Conversely, Zn, As, and Cd exhibited elevated levels over the ocean during summer, particularly in the highly polluted sample SU005, which was caused by a severe pollution event, will be discussed in detail in another manuscript on case studies.

Seasonally, concentrations of Al, Fe, Mn, and Ba over the BS and YS in spring were 4–35 times and 2–7 times higher than those in summer, respectively. This distinct seasonality can be attributed to dust storms, a frequent phenomenon in northern China during spring (Li et al., 2019). In contrast, Zn, As, and Cd displayed even higher concentrations in summer than in spring, likely related to heavily polluted samples collected. Conversely, V, Pb, and Ni exhibited no discernible seasonal variations, likely due to the consistent anthropogenic emissions such as industrial or traffic emissions (Wu et al., 2017). In Qingdao, concentrations of all these elements were notably higher in spring compared to summer (Fig.2c).

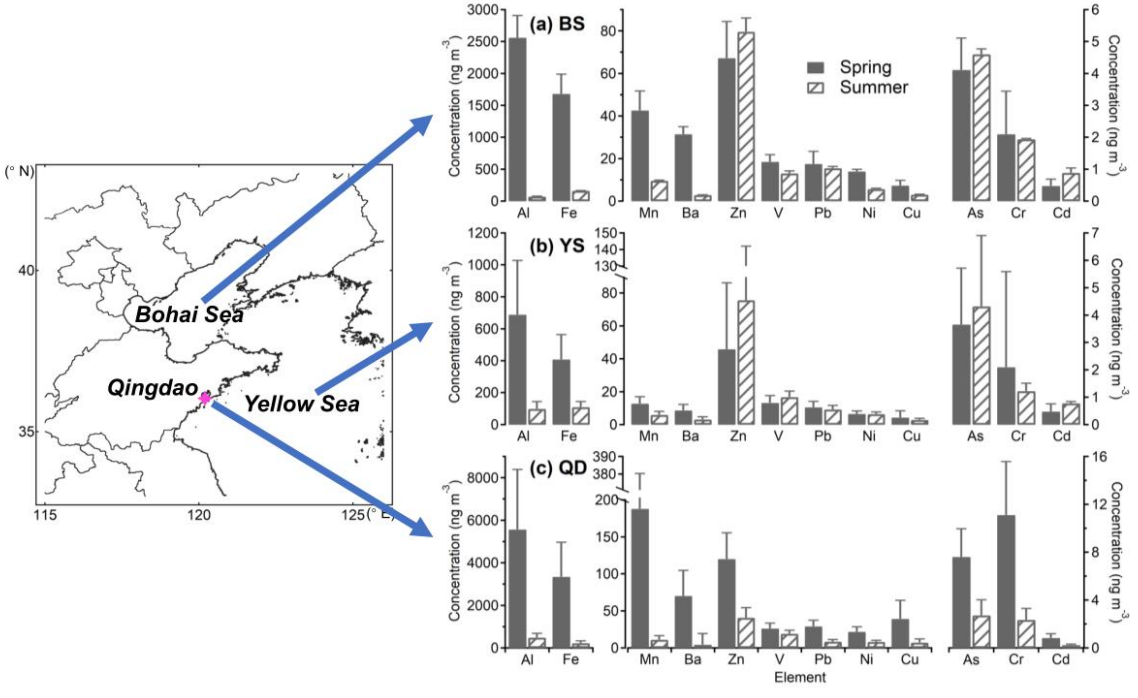

Figure 2: Concentrations of trace elements (ng m^{-3}) over the (a) BS, (b) YS, and (c) Qingdao during the campaigns in 2018. Error bars represent half of standard deviation.

https://doi.org/10.5194/egusphere-2025-4005
Preprint. Discussion started: 9 September 2025

We compared our results to other literature data on the concentrations of selected elements in various oceanic regions and typical megacities in China (Tables S4 and S5) (Qi and Zhou, 2021). Notably, elemental concentrations over the YS in this study were significantly lower than those observed during spring 2011 (Zhao et al., 2015), likely reflecting the effectiveness of emission control policies and environmental remediation measures. When comparing with spring 2018 ECS sampling data (Sun et al., 2022), a distinct north-to-south decline in the concentrations of mineral elements (Al, Fe, Mn, Ba) and anthropogenic heavy metals (e.g., Zn, Pb) was observed. This spatial pattern suggests that both dust-derived and anthropogenic pollutants, transported via the westerly winds, exert progressively weaker influences on marine aerosols from northern to southern coastal regions (Zhao et al., 2015). Only a few measurements in island were collected in summer (Yuan et al., 2023), and among all these data, extremely high Zn and Cd pollution over the BS and YS was observed and attributed to anthropogenic emissions in the Circum-Bohai-Sea (CBS) region (A geographic area encompassing the land and coastal zones surrounding the BS in China) (Polissar et al., 2001).

In Qingdao, most crustal elements, such as Fe and Mn, exhibited higher concentrations in spring and lower concentrations in summer than the annual average concentrations reported in Beijing, Shanghai, and Guangzhou, the typical megacities in China (Table S5) (Chen et al., 2008; Yang et al., 2011). Anthropogenic elements such as Zn, Pb, As, Cr, and Cd were consistently at lower levels in Qingdao than in the three megacities, indicating less anthropogenic pollution. V concentrations in Qingdao were 2–3 times higher than those in Shanghai (Chen et al., 2008), suggesting more severe pollution from ship emissions or other residual oil combustions. However, the differences in sampling times need consideration. Sect. 4.2.3 explores the impact of vessel emission control policies on the ship emission aerosols.

4 Discussions

4.1 Source apportionment of $PM_{2.5}$

Eight factors were identified by PMF. The resolved factor profiles are presented in Fig.3. The mean concentrations and the relative contributions of each factor are displayed in Fig.4. The characteristics of the determined aerosol sources are as follows. Factor 1 was identified as the secondary nitrate factor, characterized by high loadings of NO_3^-, NH_4^+ and Cl^- (Fig.3) (Wu et al., 2017; B. Xu et al., 2023). This factor contributed a significant proportion of fine particles in both coastal and marine environments, accounting for 30.5% and 15.7% of $PM_{2.5}$ mass respectively (Fig.4b). Notably, Factor 1 displayed an enhanced influence during nighttime (Fig.S4) and a significant correlation with NO_2 ($r = 0.47$, $p < 0.01$) and CO ($r = 0.37$, $p < 0.01$; Table S6). This could potentially be indicative of the nocturnal heterogeneous reaction formation or subsequent regional transport (Wang et al., 2018).

https://doi.org/10.5194/egusphere-2025-4005
Preprint. Discussion started: 9 September 2025

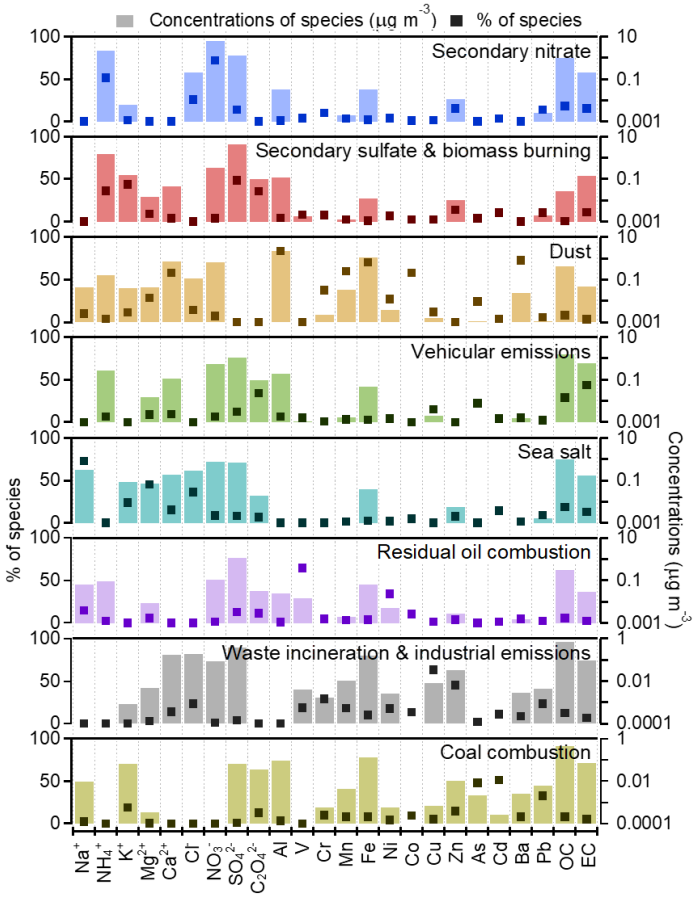

Figure 3: PMF resolved source profiles (dark points represent the percentages and light rectangles represent the concentrations of each species in each factor) of the 8-factor solution.

Factor 2 was recognized as the secondary sulfate and biomass burning (sulfate & BB) factor, marked by high SO_4^{2-}, K^+, NH_4^+ and oxalate (Wu et al., 2017; B. Xu et al., 2023). This factor accounted for 19.3% and 26.6% of the $PM_{2.5}$ mass in coastal and marine regions respectively. The notable presence of K+, oxalate, and some EC and Zn in this factor suggested the possible mixing with emissions from biomass burning (Wang et al., 2018; Zhu et al., 2022). Factor 2 exhibited significant correlations with CO ($r = 0.55$, $p < 0.01$) and RH ($r = 0.39$, $p < 0.01$). CO serves as a key tracer of primary incomplete combustion processes (Zhang et al., 2017). The strong interconnection between sulfate and oxalate can be ascribed to their similar liquid phase formation mechanisms (Yu et al., 2005; Zhou et al., 2015)..

Factor 3, identified as the dust factor, was characterized by high loadings of crustal species, including Al, Ba, Fe, Mn and Ca2+ (Fig.3) (Amil et al., 2016; Gugamsetty et al., 2012; Mustaffa et al., 2014). A significant portion of Co was also apportioned to Factor 3, denoting its crustal and anthropogenic origins. The mass ratios of Fe/Ca and Mn/Ca were 1.57 and 0.05, respectively, aligning with the typical ranges found in natural soil and paved road dust (0.8–2.6 for Fe/Ca and 0.01–0.08 for Mn/Ca) (Ho et al., 2003; Wang et al., 2018). In Qingdao, the time series of Factor 3 exhibited distinct peaks on 29–30

https://doi.org/10.5194/egusphere-2025-4005
Preprint. Discussion started: 9 September 2025

March, 3, 6, 10–11, and 15 April 2018 (Fig.S5a), each coinciding with documented springtime Asian dust events (Li et al., 2023; Li et al., 2019). Diurnally, Factor 3 exhibited a positive correlation with WS ($r = 0.42$, $p < 0.05$) and displayed an inverse correlation with RH ($r = –0.72$, $p < 0.01$; Table S6) at the coastal site in spring. These correlations suggested the influence of meteorological conditions, consistent with the inherently arid nature of dusty air masses. Factor 3 accounted for 17.8% of the total PM2.5 mass at coastal site and diminished to 4.0% within the marine environments (Fig.4b).

Factor 4 was identified as the vehicular emissions factor, characterized by significant apportionments for EC and OC, contributing 11.9% to the total coastal aerosol mass and 18.5% to the marine aerosols. OC and EC are major pollutants stemming from gasoline and diesel combustion (Liu et al., 2016; Liu et al., 2020). The presence of Cu and Zn was likely due to additives in motor oil, fuel/lubricant combustion, brake linings and tire wear (Lee et al., 2006; Pant and Harrison, 2013). During summertime, vehicular emissions demonstrated a positive correlation with NO_2 ($r = 0.82$, $p < 0.01$) and CO ($r = 0.32$, $p < 0.05$), along with a negative correlation with O_3 ($r = –0.35$, $p < 0.01$). These relationships underscored the chemical interplay where O_3 is reduced by NO to generate NO_2.

Factor 5 was characterized by high concentrations of sea salt components, including Na^+, Mg^{2+} and Cl^-, and showed good correlations with WS ($r = 0.39$, $p < 0.01$) and an inverse relationship with RH ($r = –0.58$, $p < 0.01$) (Sharma et al., 2016; Zhang et al., 2018). This factor aligned with the generation of sea salt aerosols via wind-induced disturbance on the ocean surface (Prijith et al., 2014). At the coastal site, the augmented concentrations during the daytime aligned with the sea-land breeze patterns (Fig.S4). Time series analysis indicated that Factor 5 had a prevalent influence over the marine area (Fig.S5). The peaks in the Factor 5 time series, paralleled to those of Factor 3, may imply the mixing of sea salt and dust or the influence of reverse-transport dust passing over the YS and BS (Li et al., 2023). On average, the sea salt factor contributed 8.3% to coastal $PM_{2.5}$ and 20.1% to marine $PM_{2.5}$.

Factor 6, the residual oil combustion factor, was characterized by high apportionments of V and Ni (Wu et al., 2020), contributing 4.5% and 9.0% to the total $PM_{2.5}$ mass at the coastal site and marine areas, respectively. The cargo handling capacity of Qingdao port reached 542.5 million tons in 2018, ranking fourth among the main ports of China (data obtained from China Statistical Yearbook, 2018, https://data.stats.gov.cn/easyquery.htm?cn=C01). The contributions of Factor 6 highlighted the significant influence of shipping traffic on both the coastal city and the offshore areas. A positive correlation with SO_2 ($r = 0.40$, $p < 0.01$) (Table S6) further validated its association with ship emissions (Zhang et al., 2019b).

Factor 7 was defined as the waste incineration & industrial emissions factor (WI & IE). It exhibited substantial loadings of heavy metals such as Cu, Zn, Cr, Pb, along with some Cl^-, which are tracers of waste incineration and industrial activities, including metallurgical smelting, oil mining, and the production of cement, plastic, pigment, chemical and building materials (Borai et al., 2002; Karar et al., 2006; Li et al., 2012; Tian et al., 2012; Wang et al., 2018). Its strong correlations with NO_2 ($r = 0.52$, $p < 0.01$) and SO_2 ($r = 0.29$, $p < 0.05$) underscored its industrial origins, although it is a minor contributor to total $PM_{2.5}$ (5.5% at coastal and 0.9% in the marine area, as shown in Table S6).

Factor 8 was identified as the coal combustion factor, characterized by abundances of As, Pb and Cd (Chang et al., 2018; Li et al., 2020; Rai et al., 2016; Zhang et al., 2011; Zhang et al., 2008), contributing merely 2.1% and 5.0% to the total $PM_{2.5}$

https://doi.org/10.5194/egusphere-2025-4005
Preprint. Discussion started: 9 September 2025

mass at coastal and marine areas, respectively. A notable correlation with SO_2 ($r = 0.39$, $p < 0.01$) confirmed its association with coal combustion-related activities (Lin et al., 2022).

4.2 Variation in source contributions of $PM_{2.5}$ between coastal and marine environments

4.2.1 Spring westerly transport enhances anthropogenic inputs in marine areas

Distinct differences in $PM_{2.5}$ source apportionment were observed between the coastal and marine environments during spring. Secondary nitrate, dust, and WI & IE exhibited significantly lower concentrations and relative contributions in marine environments compared to the coastal site. Specifically, secondary nitrate was the predominant contributor at the coastal site, accounting for 35.7% (19.2 μg m^{-3}) of $PM_{2.5}$ mass. In contrast, its contribution was notably lower, at 23.4% (5.2 μg m^{-3}), in the marine area (Fig.4). This disparity was driven by the divergence in the air masses transport pathways. Air masses arriving at the coastal site (spring clusters E, S, W and summer cluster L) contained higher concentrations of secondary components like NO_3^- and NH_4^+ (land-based species), which did not fully extend to marine areas (Fig.S6a and c, and Table S7). As NO_3^- and NH_4^+ are primarily associated with terrestrial sources, their influence is more significant in coastal areas.

Dust, the second largest contributor in spring, accounted for 25.2% (13.6 μg m^{-3}) at the coastal site but sharply reduced to 6.3% (1.4 μg m^{-3}) over the marine area. Dust particles with larger diameters are more likely to be removed through inertial and gravitational settling processes during transport (Gu et al., 2011; Vu et al., 2015; Zhao et al., 2015), leading to the rapid sedimentation and reduced concentration in remote marine environments (Baker & Jickells, 2006; Ma et al., 2023). The WI & IE factor also showed lower contributions in the marine area (1.2%) compared to the coastal site (6.9%), with time series peaks closely resembling those of the dust factor (Fig.S5a). It is hypothesized that during dust events, WI & IE pollutants from the Beijing-Tianjin-Hebei (BTH) region may mix with the transported dust and deposit on land, causing only a minor portion of WI & IE to reach the marine area. In contrast, sea salt was the only factor with higher relative contributions and absolute concentrations in the marine area (28.9%; 6.46 μg m^{-3}) compared to the coastal site (10.5%; 5.66 μg m^{-3}), reflecting its marine origin.

Sulfate & BB, coal combustion, vehicular emissions and residual oil combustion showed higher contributions in the marine area, despite having lower or comparable absolute concentrations to the coastal site (Fig.4). On the one hand, increased RH in marine atmosphere favored the formation of sulfate and oxalate through liquid-phase reactions (Zhang et al., 2019a; Zhou et al., 2015), enhancing their contribution in the marine atmosphere (3.8–18.5%) compared to the coastal site (2.6–7.8%). On the other hand, small-sized particles from biomass burning and coal combustion are more effectively transported to marine areas (Gu et al., 2011; Vu et al., 2015). The vehicular emissions, accounting for 18.5% in marine areas (Fig.4b), had nearly identical average concentrations in both coastal and marine environments (4.14 and 4.19 μg m^{-3}, respectively) (Fig.4a). Characterized by small EC-rich particles , these vehicular emissions can be easily transported to remote areas (Gu et al., 2011; Vu et al., 2015). As shown in Figs.S2 and S5a, time series peaks of this factor over the ocean coincided with the samples collected from air masses originating in northern and central China, i.e., samples SP010, SP014, and SP017. Residual oil combustion exhibited

https://doi.org/10.5194/egusphere-2025-4005
Preprint. Discussion started: 9 September 2025

similar average concentrations in marine (1.84 μg m^{-3}) and coastal (2.03 μg m^{-3}) areas, indicating the influence of ships and ports emissions on coastal urban areas. Unlike the WI & IE factor, these four anthropogenic factors demonstrated that varying transport paths and potential mixing with dust could affect deposition rate and land-sea distribution of anthropogenic pollutants.

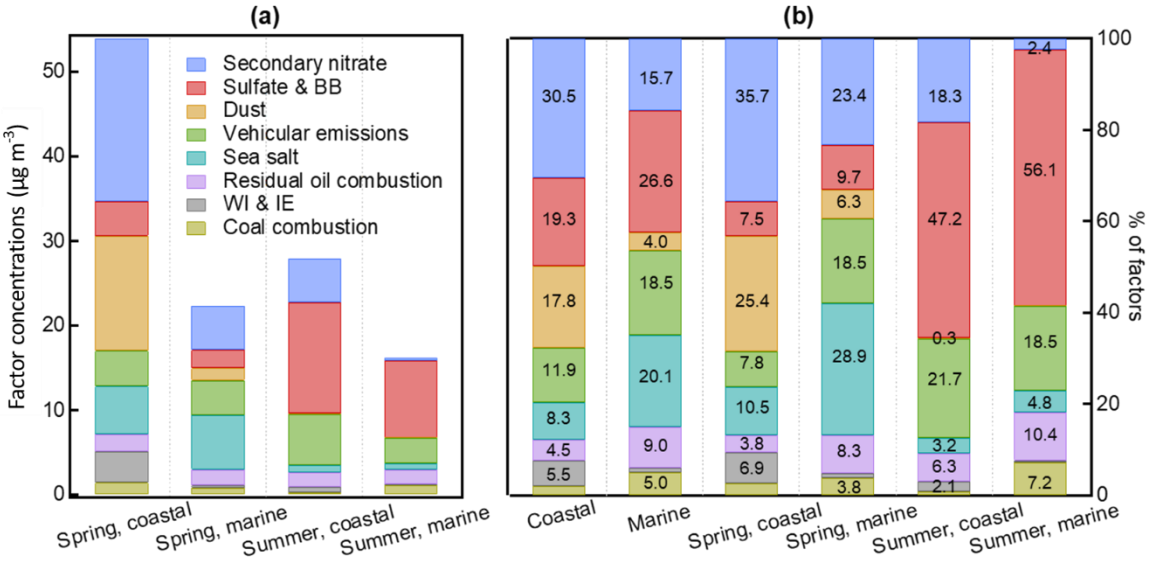

Figure 4: The averaged (a) concentrations and (b) relative percentage contributions (volume-weighted, hereafter) of identified source factors to $PM_{2.5}$ as determined by PMF analysis. Sulfate & BB refers to sulfate & biomass burning. WI & IE denotes waste incineration & industrial emissions.

4.2.2 Summer biomass burning and coal combustion dominate marine emissions

Similar spatial land-sea distribution patterns were observed for secondary nitrate, dust, WI & IE, as well as sulfate & BB in summer. However, the dominant contributor shifted from secondary nitrate in spring to sulfate & BB in summer, indicating decreased nitrate contributions during the warmer season. This reduction was attributed to the thermal decomposition of NH_4NO_3 under high summer temperatures and enhanced secondary sulfate facilitated by photochemical reactions with the high temperature and sufficient light (Wu et al., 2017).

Unlike in spring, summer data revealed higher concentrations and contributions of vehicular emissions at the coastal site (6.05 μg m^{-3}, 21.7%) compared to the marine areas (3.00 μg m^{-3}, 18.5%) (Fig.4). This difference could be ascribed to the seasonal variations in pollutants transport direction, driven by the summer southeasterly winds, altering typical land to sea trajectories. Similarly, sea salt concentrations were slightly higher at the coastal site (0.88 μg m^{-3}) compared to marine areas (0.78 μg m^{-3}), suggesting that summer southeasterly winds facilitate marine aerosol transfer inland, thereby influencing the air quality of coastal urban areas (Fig.S6c and d).

The coal combustion factor also showed a more pronounced contribution over the marine area (1.17 μg m^{-3}, 7.2%) than at the coastal site (0.26 μg m^{-3}, 0.9%). This variation was attributed to significantly elevated concentrations of trace elements in marine aerosols during summer, with one particularly polluted sample (SU005) collected over the YS (Fig.S3b). As shown in

https://doi.org/10.5194/egusphere-2025-4005
Preprint. Discussion started: 9 September 2025

Fig.S6d, the air mass corresponding to this sample mainly originated from the vicinity of the CBS region, indicating that the pollution could be traced to local or regional sources, which led to elevated pollution levels in the marine area for this air mass type, as depicted by the light blue bar in Fig.S6d.

4.2.3 Changes over the past decade

Comparative analysis of particulate matter source apportionment in Qingdao over the past decade reveals notable shifts in source contributions (Wu et al., 2017). The fraction attributed to secondary nitrate increased from 25.2% to 30.5%, suggesting a growing influence of this factor. Conversely, the sulfate (& BB) factor declined from 25.7% to 19.3%, whereas vehicular emissions demonstrated a moderate increase from 10.0% to 11.9%, accompanied by an elevation in the mass concentrations of Ni and V. These changes reflect the impacts of evolving environmental regulations and the transformation in the energy structure over the past decade.

Another interesting trend is the contribution from residual oil combustion. As a coastal city, Qingdao experiences heavy shipping traffic. Results from a PMF analysis conducted from August 2018 to May 2019 near the Qingdao Port indicated that marine vessel emissions were the primary contributor (25.1%), with the YS and BS as potential source regions (Bie et al., 2021). In this study, residual oil combustion accounted for 4.5% at the coastal background site and 9.0% over the marine area. The cargo handling capacity of Qingdao ports in 2017 was approximately double that of 2007 (China Statistical Yearbook, 2018 and 2008, https://data.stats.gov.cn/easyquery.htm?cn=C01), underscoring the significant impact of ship emissions.

The implementation of "domestic emission control areas" (DECAs) in China signified a significant regulatory shift to address air quality concerns. Commencing on January 1, 2017, ships berthed at core ports in three designated regions (the Pearl River Delta, the Yangtze River Delta, and the Bohai Rim) were mandated to use fuel with a sulfur content not exceeding 0.5% (DECA 1.0) (Zhang et al., 2019b). This regulation was further expanded on January 1, 2019 to require vessels operating within 12 nautical miles of the coastline to adhere to the same low sulfur criteria (DECA 2.0) (Yu et al., 2021). The transition to low-sulfur fuels led to a significant increase in the Ni/V ratio of emitted aerosols. In Shanghai, the Ni/V ratio in ship emitted particles derived from PMF increased from 0.34 to 0.45 between DECA 1.0 and DECA 2.0, reaching 2.14 in 2020 (Yu et al., 2021). In the present study, the measured Ni/V ratios averaged 0.83 in spring and 0.43 in summer $PM_{2.5}$, with an estimated value of 0.35 for ship-emitted aerosols by PMF. The measured Ni/V ratio observed in spring may be attributed to atmospheric dust serving as a source of Ni, whereas the estimated ratio of 0.35 aligns with the range observed during DECA 1.0. Notably, Bie et al. (2021) reported a Ni/V ratio as high as 2.17 in 2019 near the Qingdao Port, providing evidence of the effectiveness of DECA policy measures. Furthermore, stricter emission controls onshore compared to those implemented at sea could explain the observed variations in Ni/V ratios, highlighting the importance of comprehensive emission management strategies to address regional air quality challenges.

https://doi.org/10.5194/egusphere-2025-4005
Preprint. Discussion started: 9 September 2025

4.3 Source contributions of individual elements

This study revealed clear disparities in the source contributions to the ten essential elements across terrestrial and marine regions, mirroring the spatial distribution patterns seen in PM2.5 (Fig.5 and Table S8). The influence of dust and WI & IE sources decreased, whereas coal combustion, vehicular emissions and sea salt exhibited enhanced contributions to elements over the marine area.

4.3.1 Fe, Mn and Cr

Atmospheric aerosols containing Fe and Mn are crucial for marine biogeochemistry and ecosystem dynamics. As a limiting nutrient, Fe is closely coupled with sulfur cycles in both the atmosphere and ocean, triggering phytoplankton blooms, and enhancing carbon dioxide (CO_2) sequestration through the global carbon cycle (Shi et al., 2012; Zhuang et al., 1992). Similarly, Mn serves as an essential cofactor for enzymes involved in photosynthesis and other biochemical processes, making it vital for marine organisms, and its deficiency directly impacts the growth rate of phytoplankton (Morel & Price, 2003; Hawco et al., 2022).

In spring, dust was the dominant source of Fe and Mn at the coastal city, contributing 77.8% and 67.9% to the total Fe and Mn, respectively (Fig.5a and b). However, marine aerosols exhibited significantly increased contributions from vehicular emissions (6.7% and 7.9% for Fe and Mn, respectively) and coal combustion (19.7% and 20.3%). In summer, coal combustion became the primary contributor to marine Fe and Mn (58.3% and 51.2%, respectively), exceeding coastal contributions by 4–5 times. This shift highlights the long-range transport of fine anthropogenic particles to marine regions, enriching aerosols with pollution-derived elements. These findings align with previous studies: Chen et al. (2024) reported dust as the predominant source of Fe (88%) in Qingdao during spring (Chen et al., 2024), while Zhang et al. (2024) observed substantial contributions from both dust (68.6%) and coal combustion (21.2%) in the YS, ECS, and Northwest Pacific. The findings regarding Mn in Beijing align with our analysis for Qingdao, where dust served as the primary source during spring, but shifted to industrial emissions in summer (Yang et al., 2022). Notably, anthropogenic Fe typically exhibited higher solubility (Sun et al., 2024), which may enhance its bioavailability in marine aerosols. Furthermore, sea salt contributed 11.3% to Fe and 7.9% to Mn in marine aerosols during spring, suggesting mixing between crustal species or Fe/Mn from other sources with sea spray aerosols (SSAs) (Geng et al., 2014; Hilario et al., 2020). Scanning electron microscopy (SEM) analysis by Geng et al. (2014) confirmed the blending of dust and SSAs, supporting this mechanism. This mixing phenomenon may also accelerate the dissolution of Fe in the particles.

Cr followed a similar source pattern to Fe and Mn in spring (Fig.5c), with secondary nitrate and sulfate & BB contributing more significantly in both seasons. However, marine aerosols exhibited a pronounced increase in coal combustion contributions (25.6% in spring and 42.9% in summer) compared to coastal particles, likely due to emissions from coastal power plants transported seaward. WI & IE was the second most significant contributor to Cr in Qingdao, consistent with

https://doi.org/10.5194/egusphere-2025-4005
Preprint. Discussion started: 9 September 2025

Yang et al. (2022), who reported industrial emissions contributions of 41%–77% in Beijing, slightly higher than our findings (31.0% in spring, 25.6% in summer).

4.3.2 Ni, Cu, Zn, V and Cd

Ni, Cu, Zn, and Cd can influence phytoplankton growth dynamics, modify marine biotic community structure, and affect carbon sequestration processes, functioning either as enzyme cofactors or structural elements in proteins (Jickells et al., 2005; Morel and Price, 2003; Shelley et al., 2015). Notably, Ni and V primarily originated from residual oil combustion, with contributions being markedly higher over the marine area (58.6–84.4%) compared to the coastal site (23.3–66.6%) (Fig.5d and e). Over the marine area, sulfate & BB (2.0–11.8%), coal combustion (14.1–27.4%) and industrial emissions (42.0–42.9%) contributed more significantly to Cu (Fig.5f). In Qingdao, WI & IE was the predominant source of Cu, which is consistent with observations in Beijing (Yang et al., 2022). Apart from the contributions of sea salt, Zn originated from various anthropogenic sources including waste incineration, industrial emissions, coal combustion and secondary aerosol formation. In the marine area, coal combustion dominated Zn contributions, accounting for 26.9% and 40.8% of total Zn during spring and summer, respectively (Fig.5g).

4.3.3 Pb, Cd and As

Pb, Cd, and As, which are biologically toxic, pose potential non-carcinogenic or carcinogenic risks to human health and cause considerable detriment upon marine ecosystems (Nagajyoti et al., 2010; Zhang et al., 2018). Source apportionment revealed that coal combustion was the dominant contributor of Pb and Cd in marine areas, particularly during summer, accounting for 65.8% of Pb and 74.5% of Cd (Fig.5h and i). In Beijing, the predominant sources of Pb were coal combustion in spring and industrial emissions in summer (Yang et al., 2022), mirroring our coastal observations. Similarly, coal combustion was identified as the primary source of As (26.4–75.5%), with its influence increasing over the marine areas during spring (61.4%) and summer (75.5%) (Fig.5j). The emission inventory also indicates that 74.2% of As emissions can be ascribed to coal combustion in China (Tian et al., 2015). Furthermore, vehicular emissions also contributed significantly to As (13.0–57.8%). Notably, the remarkably elevated levels of Zn, Pb, Cd and As in the summer sample SU005 were attributed to the enhanced contributions from coal combustion across the BS and YS, accounting for 54.3% of Zn, 76.8% of Pb, 83.2% of Cd and 78.6% of As in this sample (Fig.S5b). Another interesting finding was the significant contribution of sea salt to Zn, Pb and Cd in marine environments during spring, indicating the mixing between SSAs and anthropogenic aerosols. The time series suggested that the peaks in sea salt contributions coincided with the high concentrations of Pb, Cd and Zn (Figs.S3a and S5a).

https://doi.org/10.5194/egusphere-2025-4005
Preprint. Discussion started: 9 September 2025

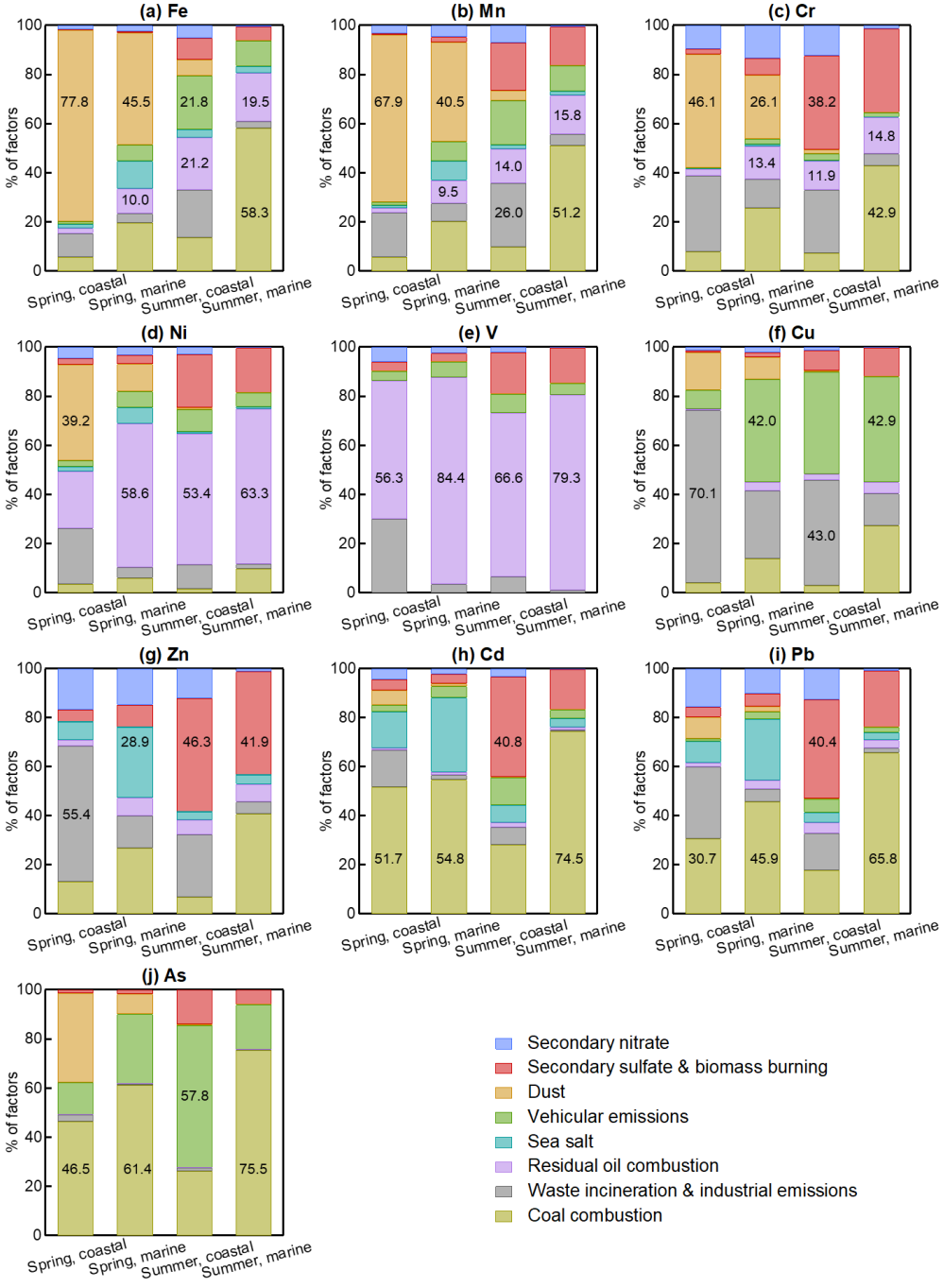

385 **Figure 5: Percentage contributions of various source factors to individual elements based on PMF results.**

https://doi.org/10.5194/egusphere-2025-4005
Preprint. Discussion started: 9 September 2025

5 Conclusions

This study investigated the spatial and seasonal distributions in $PM_{2.5}$ sources and associated trace elements in Qingdao and its adjacent offshore areas of the Bohai and Yellow Seas during spring and summer 2018, delving into land-sea contrasts and the influence of anthropogenic activities on the offshore marine air. Eight aerosol sources were identified in coastal and offshore regions, including secondary nitrate, the mixture of secondary sulfate and biomass burning, dust, vehicular emissions, sea salt, residual oil combustion, coal combustion, and the mixture of waste incineration and industrial pollutants.

We observed distinct terrestrial-marine gradients in aerosol sources driven by atmospheric processes. Secondary nitrate, primarily derived from terrestrial anthropogenic activities, declined sharply from land to marine areas by 35.7% to 18.3% in spring, and by 23.4% to 2.4% in summer. In contrast, secondary sulfate and biomass burning contributions increased in marine environments from 7.5% and 9.7% over land to 47.2% and 56.1% over the ocean in spring and summer, respectively, which are attributable to enhanced sulfur precursor availability and long-range transport. Natural terrestrial sources, including dust and dust-anthropogenic mixtures, demonstrated pronounced attenuation over marine areas due to size-dependent particle settling. For example, dust contributions declined from 25.2% on land to 6.3% over the marine areas in spring. In contrast, finer anthropogenic particulates, such as vehicular emissions, exhibited enhanced offshore transport (18.5% marine vs. 7.8% coastal in spring). Summer southerly winds moderated this marine-land contrast. Marine-derived aerosols, particularly sea salt and ship emissions, dominated oceanic sectors, with ship emissions contributing up to 8.3% in spring and 10.4% in summer.

In terms of the trace elements, all exhibited notably higher concentrations in Qingdao compared to marine areas in spring. In contrast, Zn, As, and Cd levels were higher in oceanic regions in summer. Elemental transport reflected aerosol behavior but exhibited source-specific nuances. Springtime terrestrial dominance (Fe, Mn, Cr, Ni: 39.2–77.8% land vs. 11.2–45.5% offshore, primarily from dust) shifted to summer marine coal combustion dominance (Fe: 58.3%, Mn: 51.2%, Cr: 42.9%), reflecting enhanced anthropogenic influence. Springtime marine environments also showed elevated sea salt contributions to Fe, Mn, Zn, Cd, and Pb (7.9–30.2%), suggesting synergistic dust–anthropogenic interactions. This interplay may facilitate mineral dissolution, particularly for Fe and Mn, amplifying their biogeochemical reactivity in marine ecosystems. Ship emissions enriched oceanic Ni and V, with contributions of 58.6% and 84.4% in spring and 63.3% and 79.3% in summer, respectively, compared to terrestrial levels (23.3% and 56.3% in spring and 53.4% and 66.3% in summer), highlighting maritime anthropogenic impacts.

These findings underscore the complex interplay of natural and anthropogenic drivers in shaping coastal aerosol composition, emphasizing the critical role of atmospheric transport and source-receptor dynamics in influencing aerosol-borne element distributions and interactions between continental and marine aerosols.

https://doi.org/10.5194/egusphere-2025-4005
Preprint. Discussion started: 9 September 2025

Data availability. The backward trajectories were calculated using the Hybrid Single-Particle Lagrangian Integrated Trajectory (HYSPLIT) transport model (https://www.ready.noaa.gov/HYSPLIT.php). The data associated with the figures in this manuscript, including Supporting Materials, are available in the in-text data citation reference Zhou (2025).

Author contribution.

Yuxuan Qi: formal analysis, writing-original draft, validation, writing-review & editing; **Wenshuai Li:** investigating, formal analysis, validation; **Wen Qu:** methodology; **Haizhou Zhang:** methodology; **Wenqing Zhu:** investigating, formal analysis, validation; **Jinhui Shi:** writing-review & editing, methodology; **Daizhou Zhang:** validation, writing-review & editing; **Yanjing Zhang:** investigation, validation; **Lifang Sheng:** validation, writing-review; **Wencai Wang:** validation, writing-review; **Yunhui Zhao:** investigation, validation; **Yuanyuan Ma:** investigation, validation; **Danyang Ren:** investigation, validation; **Guanru Wu:** investigation, validation; **Xinfeng Wang:** methodology; **Xiaohong Yao:** validation, methodology; **Yang Zhou:** conceptualization, writing-review & editing, validation, funding acquisition, supervision, project administration.

Competing interests. The authors declare that they have no conflict of interest.

Acknowledgments.

This research was sponsored by the National Natural Science Foundation of China (NSFC) (No. 42475119 and 41605114) and Shandong Provincial Natural Science Foundation (No. ZR2024MD016). The authors would like to thank all the colleagues who participated in these campaigns for their support. Data acquisition and sample collections were supported by NSFC Open Research Cruise (Cruise No. NORC2018-001), funded by Shiptime Sharing Project of NSFC. This cruise was conducted onboard R/V *DONGFANGHONG 2* by Ocean University of China. The authors gratefully acknowledge the NOAA-ARL for providing the HYSPLIT transport and dispersion model.

References

Amil, N., Latif, M. T., Khan, M. F., and Mohamad, M.: Seasonal variability of PM2.5 composition and sources in the Klang Valley urban-industrial environment, Atmos. Chem. Phys., 16, 5357-5381, https://doi.org/10.5194/acp-16-5357-2016, 2016.

Baker, A. R., and Jickells, T. D.: Mineral particle size as a control on aerosol iron solubility. Geophys. Res. Lett., 33, L17608. https://doi.org/10.1029/2006GL026557, 2006.

Baker, A. R., Jickells, T. D., Witt, M., and Linge, K. L.: Trends in the solubility of iron, aluminium, manganese and phosphorus in aerosol collected over the Atlantic Ocean, Mar. Chem., 98, 43-58, https://doi.org/10.1016/j.marchem.2005.06.004, 2006.

Bie, S., Yang, L., Zhang, Y., Huang, Q., Li, J., Zhao, T., Zhang, X., Wang, P., and Wang, W.: Source appointment of PM2.5 in Qingdao Port, East of China, Sci. Total. Environ., 755, https://doi.org/10.1016/j.scitotenv.2020.142456, 2021.

https://doi.org/10.5194/egusphere-2025-4005
Preprint. Discussion started: 9 September 2025

Borai, E. H., El-Sofany, E. A., Abdel-Halim, A. S., and Soliman, A. A.: Speciation of hexavalent chromium in atmospheric particulate samples by selective extraction and ion chromatographic determination, Trac-Trend. Anal. Chem., 21, 741-745, https://doi.org/10.1016/S0165-9936(02)01102-0, 2002.

Boyd, P. W., Watson, A. J., Law, C. S., Abraham, E. R., Trull, T., Murdoch, R., Bakker, D. C. E., Bowie, A. R., Buesseler, K. O., Chang, H., Charette, M., Croot, P., Downing, K., Frew, R., Gall, M., Hadfield, M., Hall, J., Harvey, M., Jameson, G., LaRoche, J., Liddicoat, M., Ling, R., Maldonado, M. T., McKay, R. M., Nodder, S., Pickmere, S., Pridmore, R., Rintoul, S., Safi, K., Sutton, P., Strzepek, R., Tanneberger, K., Turner, S., Waite, A., and Zeldis, J.: A mesoscale phytoplankton bloom in the polar Southern Ocean stimulated by iron fertilization, Nature, 407, 695-702, https://doi.org/10.1038/35037500, 2000.

Buck, C. S., Landing, W. M., and Resing, J. A.: Particle size and aerosol iron solubility: A high-resolution analysis of Atlantic aerosols, Mar. Chem., 120, 14-24, https://doi.org/10.1016/j.marchem.2008.11.002, 2010.

Chang, Y., Huang, K., Xie, M., Deng, C., Zou, Z., Liu, S., and Zhang, Y.: First long-term and near real-time measurement of trace elements in China's urban atmosphere: Temporal variability, source apportionment and precipitation effect. Atmos. Chem. Phys., 18, 11793-11812. https://doi.org/10.5194/acp-18-11793-2018, 2018.

Chen, J., Tan, M., Li, Y., Zheng, J., Zhang, Y., Shan, Z., Zhang, G., and Li, Y.: Characteristics of trace elements and lead isotope ratios in PM2.5 from four sites in Shanghai, J. Hazard. Mater., 156, 36-43, https://doi.org/10.1016/j.jhazmat.2007.11.122, 2008.

Choobari, O. A., Zawar-Reza, P., and Sturman, A.: The global distribution of mineral dust and its impacts on the climate system: A review, Atmos. Res., 138, 152-165, https://doi.org/10.1016/j.atmosres.2013.11.007, 2014.

Draxler, R. R., & Rolph, G. D.: HYSPLIT (HYbrid Single-Particle Lagrangian Integrated Trajectory) Model access via NOAA ARL READY Website, last, NOAA Air Resources Laboratory, College Park, MD, 2014.

Falkowski, P. G., Barber, R. T., and Smetacek, V.: Biogeochemical controls and feedbacks on ocean primary production, Science, 281, 200-206, https://doi.org/10.1126/science.281.5374.200, 1998.

Gen, M., Zhang, R., and Chen, C. K.: Nitrite/Nitrous Acid Generation from the Reaction of Nitrate and Fe(II) Promoted by Photolysis of Iron-Organic Complexes. Environ. Sci. Technol., 55, 15715-15723. https://doi.org/ 10.1021/acs.est.1c05641, 2022.

Geng, H., Hwang, H., Liu, X., Dong, S., & Ro, C. U.: Investigation of aged aerosols in size-resolved Asian dust storm particles transported from Beijing, China, to Incheon, Korea, using low-Z particle EPMA. Atmos. Chem. Phys., 14, 3307-3323. https://doi.org/10.5194/acp-14-3307-2014. 2014.

Gu, J., Pitz, M., Schnelle-Kreis, J., Diemer, J., Reller, A., Zimmermann, R., Soentgen, J., Stoelzel, M., Wichmann, H.-E., Peters, A., and Cyrys, J.: Source apportionment of ambient particles: Comparison of positive matrix factorization analysis applied to particle size distribution and chemical composition data, Atmos. Environ., 45, 1849-1857, https://doi.org/10.1016/j.atmosenv.2011.01.009, 2011.

https://doi.org/10.5194/egusphere-2025-4005
Preprint. Discussion started: 9 September 2025

Gugamsetty, B., Wei, H., Liu, C. N., Awasthi, A., Hsu, S. C., Tsai, C. J., Roam, G. D., Wu, Y. C., and Chen, C. F.: Source Characterization and Apportionment of PM10, PM2.5 and PM0.1 by Using Positive Matrix Factorization, Aerosol Air Qual. Res., 12, 476-491, https://doi.org/10.4209/aaqr.2012.04.0084, 2012.

Hawco, N. J., Tagliabue, A. & Twining, B. S.: Manganese limitation of phytoplankton physiology and productivity in the Southern Ocean. Global Biogeochem. Cycles, 36, e2022GB007382. https://doi.org/10.1029/2022GB007382, 2022.

Hilario, M. R. A., Cruz, M. T., Cambaliza, M. O. L., Reid, J. S., Xian, P., Simpas, J. B., Lagrosas, N. D., Uy, S. N. Y., Cliff, S., and Zhao, Y.: Investigating size-segregated sources of elemental composition of particulate matter in the South China Sea during the 2011 Vasco cruise, Atmos. Chem. Phys., 20, 1255-1276, https://doi.org/10.5194/acp-20-1255-2020, 2020.

Ho, K. F., Lee, S. C., Chow, J. C., and Watson, J. G.: Characterization of PM10 and PM2.5 source profiles for fugitive dust in Hong Kong, Atmos. Environ., 37, 1023-1032, https://doi.org/10.1016/S1352-2310(02)01028-2, 2003.

Hsieh, C. -C., You, C. -F., & Ho, T. -Y.: The solubility and deposition flux of East Asian aerosol metals in the East China Sea: The effects of aeolian transport processes. Mar. Chem., 253, 104268. https://doi.org/10.1016/j.marchem.2023.104268, 2023.

Hsu, S. C., Wong, G. T. F., Gong, G. C., Shiah, F. K., Huang, Y. T., Kao, S. J., Tsai, F. J., Lung, S. C. C., Lin, F. J., Lin, II, Hung, C. C., and Tseng, C. M.: Sources, solubility, and dry deposition of aerosol trace elements over the East China Sea, Mar. Chem., 120, 116-127, https://doi.org/10.1016/j.marchem.2008.10.003, 2010.

Huang, J., Wang, T., Wang, W., Li, Z., and Yan, H.: Climate effects of dust aerosols over East Asian arid and semiarid regions, J. Geophys. Res.-Atmos., 119, 11398-11416, https://doi.org/10.1002/2014JD021796, 2014.

Ito, A. and Feng, Y.: Iron mobilization in North African Dust, Earth System Science 2010: Global Change, Climate and People, WOS:000312268000004, https://doi.org/10.1016/j.proenv.2011.05.004, 2011.

Ito, A., Ye, Y., Baldo, C., & Shi, Z. B.: Ocean fertilization by pyrogenic aerosol iron. npj Clim. Atmos. Sci., 4, Article 30. https://doi.org/10.1038/s41612-021-00185-8, 2021.

Jickells, T. D., An, Z. S., Andersen, K. K., Baker, A. R., Bergametti, G., Brooks, N., Cao, J. J., Boyd, P. W., Duce, R. A., Hunter, K. A., Kawahata, H., Kubilay, N., laRoche, J., Liss, P. S., Mahowald, N., Prospero, J. M., Ridgwell, A. J., Tegen, I., and Torres, R.: Global iron connections between desert dust, ocean biogeochemistry, and climate, Science, 308, 67-71, https://doi.org/10.1126/science.1105959, 2005.

Karar, K., Gupta, A. K., Kumar, A., and Biswas, A. K.: Characterization and identification of the sources of chromium, zinc, lead, cadmium, nickel, manganese and iron in Pm-10 particulates at the two sites of kolkata, india, Environ. Monit. Assess., 120, 347-360, https://doi.org/10.1007/s10661-005-9067-7, 2006.

Kim, N., Yum, S. S., Cho, S., Jung, J., Lee, G., and Kim, H.: Atmospheric sulfate formation in the Seoul Metropolitan Area during spring/summer: Effect of trace metal ions. Environ. Pollut., 315, 120379. https://doi.org/10.1016/j.envpol.2022.120379, 2022.

Lee, J. H., Hopke, P. K., and Turner, J. R.: Source identification of airborne PM2.5 at the St. Louis-Midwest Supersite, J. Geophys. Res.-Atmos., 111, https://doi.org/10.1029/2005JD006329, 2006.

https://doi.org/10.5194/egusphere-2025-4005
Preprint. Discussion started: 9 September 2025

Li, P., Li, Q., Shi, J., Gao, H., and Yao, X.: Concentration, solubility, and dry deposition flux of trace elements in fine and coarse particles in Qingdao during summer (in Chinese), Environ. Sci., 39, 3067-3074, https://doi.org/10.13227/j.hjkx.201712231, 2018.

Li, Q., Cheng, H., Zhou, T., Lin, C., and Guo, S.: The estimated atmospheric lead emissions in China, 1990-2009, Atmos. Environ., 60, 1-8, https://doi.org/10.1016/j.atmosenv.2012.06.025, 2012.

Li, R., Wang, Q., He, X., Zhu, S., Zhang, K., Duan, Y., Fu, Q., Qiao, L., Wang, Y., Huang, L., Li, L., and Yu, J. Z.: Source apportionment of PM2.5 in Shanghai based on hourly organic molecular markers and other source tracers, Atmos. Chem. Phys., 20, 12047-12061, https://doi.org/10.5194/acp-20-12047-2020, 2020.

Li, T., Wang, Y., Li, W., Chen, J., Wang, T., and Wang, W.: Concentrations and solubility of trace elements in fine particles at a mountain site, southern China: regional sources and cloud processing, Atmos. Chem. Phys., 15, 8987-9002, https://doi.org/10.5194/acp-15-8987-2015, 2015.

Li, T., Wang, Y., Zhou, J., Wang, T., Ding, A., Nie, W., Xue, L., Wang, X., and Wang, W.: Evolution of trace elements in the planetary boundary layer in southern China: Effects of dust storms and aerosol-cloud interactions, J. Geophys. Res.-Atmos., 122, 3492-3506, https://doi.org/10.1002/2016JD025541, 2017.

Li, W., Qi, Y., Liu, Y., Wu, G., Zhang, Y., Shi, J., Qu, W., Sheng, L., Wang, W., Zhang, D., and Zhou, Y.: Daytime and nighttime aerosol soluble iron formation in clean and slightly polluted moist air in a coastal city in eastern China. Atmos. Chem. Phys., 24, 6495-6508. https://doi.org/10.5194/acp-24-6495-2024, 2024.

Li, W., Qi, Y., Qu, W., Qu, W., Shi, J., Zhang, D., Liu, Y., Wu, F., Ma, Y., Zhang, Y., Ren, D., Du, X., Yang, S., Wang, X., Yi, L., Gao, X., Wang, W., Ma, Y., Sheng, L., and Zhou, Y.: Sulfate and nitrate elevation in reverse-transport dust plumes over coastal areas of China. Atmos. Environ., 295, 119518, Article 119518. https://doi.org/10.1016/j.atmosenv.2022.119518, 2023.

Li, W., Wang, W., Zhou, Y., Ma, Y., Zhang, D., and Sheng, L.: Occurrence and Reverse Transport of Severe Dust Storms Associated with Synoptic Weather in East Asia, Atmosphere, 10, https://doi.org/10.3390/atmos10010004, 2019.

Li, Y.-X., Luo, L., Li, J.-W., Hsu, S.-C, Ni, Y.-Z., and Kao, S.-J.: Middle East and Central Asian dust reaches the South China Sea in summer. Natl. Sci. Rev., nwaf274. https://doi.org/10.1093/nsr/nwaf274, 2025.

Li, Z., Ho, K.-F., Dong, G., Lee, H. F., and Yim, S. H. L.: A novel approach for assessing the spatiotemporal trend of health risk from ambient particulate matter components: Case of Hong Kong. Environ. Res., 204, 111866. https://doi.org/10.1016/j.envres.2021.111866, 2022.

Lin, Y.-C., Yu, M., Xie, F., and Zhang, Y. Anthropogenic Emission Sources of Sulfate Aerosols in Hangzhou, East China: Insights from Isotope Techniques with Consideration of Fractionation Effects between Gas-to-Particle Transformations. Environ. Sci. Technol., 56, 3905-3914. https://doi.org/10.1021/acs.est.1c05823, 2022.

Liu, B., Song, N., Dai, Q., Mei, R., Sui, B., Bi, X., and Feng, Y.: Chemical composition and source apportionment of ambient PM2.5 during the non-heating period in Taian, China, Atmos. Res., 170, 23-33, https://doi.org/10.1016/j.atmosres.2015.11.002, 2016.

https://doi.org/10.5194/egusphere-2025-4005
Preprint. Discussion started: 9 September 2025

Liu, B., Sun, X., Zhang, J., Bi, X., Li, Y., Li, L., Dong, H., Xiao, Z., Zhang, Y., and Feng, Y.: Characterization and Spatial Source Apportionments of Ambient PM10 and PM2.5 during the Heating Period in Tian'jin, China, Aerosol Air Qual. Res., 20, 1-13, https://doi.org/10.4209/aaqr.2019.06.0281, 2020.

López-García, P., Gelado-Caballero, M. D., Collado-Sánchez, C., and Hernández-Brito, J. J.: Solubility of aerosol trace elements: Sources and deposition fluxes in the Canary Region, Atmos. Environ., 148, 167-174, https://doi.org/10.1016/j.atmosenv.2016.10.035, 2017.

Luo, C., Mahowald, N., Bond, T., Chuang, P. Y., Artaxo, P., Siefert, R., Chen, Y., and Schauer, J.: Combustion iron distribution and deposition, Global Biogeochem. Cy., 22, https://doi.org/10.1029/2007GB002964, 2008.

Luo, C. H., Wang, W. C., Sheng, L. F., Zhou, Y., Hu, Z. Y., Qu, W. J., Li, X. D., and Hai, S. F.: Influence of polluted dust on chlorophyll-a concentration and particulate organic carbon in the subarctic North Pacific Ocean based on satellite observation and the WRF-Chem simulation, Atmos. Res., 236, 104812, https://doi.org/10.1016/j.atmosres.2019.104812, 2020.

Ma, Y. N., Ma, Y. J., Zhang, X. G., Wu, F. K., Liu, Q., Wu, X. Y., Lyu, Y., Jiang, J. W., Zhao, D. D., Ren, X. B., Li, Z., Jia, X., Li, M. C., Yao, J. Y., Gao, Z. M., Hai, S. F., and Xin, J. Y. Shipboard Observations of Aerosol Chemical Properties Over the Western Pacific Ocean in Winter 2018. J. Geophys. Res.-Atmos., 128, Article e2023JD039422. https://doi.org/10.1029/2023JD039422, 2023.

Mahowald, N.: Aerosol Indirect Effect on Biogeochemical Cycles and Climate, Science, 334, 794-796, https://doi.org/10.1126/science.1207374, 2011.

Mann, E. L., Ahlgren, N., Moffett, J. W., and Chisholm, S. W.: Copper toxicity and cyanobacteria ecology in the Sargasso Sea, Limnol. Oceanogr., 47, 976-988, https://doi.org/10.4319/lo.2002.47.4.0976, 2002.

Martin, J. H.: Glacial-interglacial CO2 change: The iron hypothesis, Paleoceanography, 5, 1-13, https://doi.org/10.1029/PA005i001p00001, 1990.

Meng, Y., Li, P., Cao, W., Shi, J., Gao, H., and Yao, X.: Size distribution of particulate trace elements in mass concentration and their size-dependent solubility in the atmosphere in Qingdao, China (in Chinese), China Environ. Sci., 37, 851-858, 2017.

Ming, L., Jin, L., Li, J., Fu, P., Yang, W., Liu, D., Zhang, G., Wang, Z., and Li, X.: PM2.5 in the Yangtze River Delta, China: Chemical compositions, seasonal variations, and regional pollution events. Environ. Pollut., 223, 200-212. https://doi.org/10.1016/j.envpol.2017.01.013, 2017.

Morel, F. M. M. and Price, N. M.: The biogeochemical cycles of trace metals in the oceans, Science, 300, 944-947, https://doi.org/10.1126/science.1083545, 2003.

Mustaffa, N. I. H., Latif, M. T., Ali, M. M., and Khan, M. F.: Source apportionment of surfactants in marine aerosols at different locations along the Malacca Straits, Environ. Sci. Pollut. R., 21, 6590-6602, https://doi.org/10.1007/s11356-014-2562-z, 2014.

Nagajyoti, P. C., Lee, K. D., and Sreekanth, T. V. M.: Heavy metals, occurrence and toxicity for plants: a review. Environ. Chem. Lett., 8, 199-216. https://doi.org/10.1007/s10311-010-0297-8, 2010.

https://doi.org/10.5194/egusphere-2025-4005
Preprint. Discussion started: 9 September 2025

Norris, G., Duvall, R., Brown, S., and Bai, S.: EPA positive matrix factorization (PMF) 5.0 fundamentals and user guide, US Environmental Protection Agency Office of Research and Development, Washington, DC, https://www.epa.gov/air-research/epa-positive-matrix-factorization-50-fundamentals-and-user-guide, 2014.

Paatero, P. and Tapper, U.: Positive matrix factorization - a nonnegative factor model with optimal utilization of error-estimates of data values, Environmetrics, 5, 111-126, https://doi.org/10.1002/env.3170050203, 1994.

Pant, P. and Harrison, R. M.: Estimation of the contribution of road traffic emissions to particulate matter concentrations from field measurements: A review, Atmos. Environ., 77, 78-97, https://doi.org/10.1016/j.atmosenv.2013.04.028, 2013.

Peng, L., Cui, X., Wang, X., Guo, Y., Ma, Y., Wen, Y., Wang, Z., Guo, Y., and Sun, J. Occurrence, source, and ecological impacts of dry depositing aerosol metal elements in the Bohai Bay. Mar. Environ. Res., 208, 107137. https://doi.org/10.1016/j.marenvres.2025.107137, 2025.

Polissar, A. V., Hopke, P. K., and Poirot, R. L.: Atmospheric aerosol over Vermont: Chemical composition and sources, Environ. Sci. Technol., 35, 4604-4621, https://doi.org/10.1021/es0105865, 2001.

Prijith, S. S., Aloysius, M., and Mohan, M.: Relationship between wind speed and sea salt aerosol production: A new approach, J. Atmos. Sol.-Terr. Phy., 108, 34-40, https://doi.org/10.1016/j.jastp.2013.12.009, 2014.

Qi, Y. and Zhou, Y.: A review of the iron and its solubility in atmospheric aerosols (in Chinese), J. Mar. Meteorol., 41, 1-13, https://doi.org/10.19513/j.cnki.issn2096-3599.2021.02.001, 2021.

Qiu, S.: Solubility of iron in atmospheric aerosols and related factors in Marginal Seas, China (in Chinese), M.S. Thesis, Ocean University of China, Qingdao, China, 2015.

Rai, P., Chakraborty, A., Mandariya, A. K., and Gupta, T.: Composition and source apportionment of PM1 at urban site Kanpur in India using PMF coupled with CBPF, Atmos. Res., 178, 506-520, https://doi.org/10.1016/j.atmosres.2016.04.015, 2016.

Ramanathan, V., Ramana, M. V., Roberts, G., Kim, D., Corrigan, C., Chung, C., and Winker, D.: Warming trends in Asia amplified by brown cloud solar absorption, Nature, 448, 575-U575, https://doi.org/10.1038/nature06019, 2007.

Schroth, A. W., Crusius, J., Sholkovitz, E. R., and Bostick, B. C.: Iron solubility driven by speciation in dust sources to the ocean, Nat. Geosci., 2, 337-340, https://doi.org/10.1038/NGEO501, 2009.

Sharma, S. K., Sharma, A., Saxena, M., Choudhary, N., Masiwal, R., Mandal, T. K., and Sharma, C.: Chemical characterization and source apportionment of aerosol at an urban area of Central Delhi, India, Atmos. Pollut. Res., 7, 110-121, https://doi.org/10.1016/j.apr.2015.08.002, 2016.

Shelley, R. U., Morton, P. L., and Landing, W. M.: Elemental ratios and enrichment factors in aerosols from the US-GEOTRMES North Atlantic transects, Deep-Sea Res. Pt. II, 116, 262-272, https://doi.org/10.1016/j.dsr2.2014.12.005, 2015.

Shi, J.-H., Zhang, J., Gao, H.-W., Tan, S.-C., Yao, X.-H., and Ren, J.-L.: Concentration, solubility and deposition flux of atmospheric particulate nutrients over the Yellow Sea, Deep-Sea Res. Pt. II, 97, 43-50, https://doi.org/10.1016/j.dsr2.2013.05.004, 2013.

https://doi.org/10.5194/egusphere-2025-4005
Preprint. Discussion started: 9 September 2025

Shi, Z., Krom, M. D., Jickells, T. D., Bonneville, S., Carslaw, K. S., Mihalopoulos, N., Baker, A. R., and Benning, L. G.: Impacts on iron solubility in the mineral dust by processes in the source region and the atmosphere: A review, Aeolian Res., 5, 21-42, https://doi.org/10.1016/j.aeolia.2012.03.001, 2012.

Sholkovitz, E. R., Sedwick, P. N., Church, T. M., Baker, A. R., and Powell, C. F.: Fractional solubility of aerosol iron: Synthesis of a global-scale data set, Geochim. Cosmochim. Ac., 89, 173-189, https://doi.org/10.1016/j.gca.2012.04.022, 2012.

Sorooshian, A., Wang, Z., Coggon, M. M., Jonsson, H. H., and Ervens, B.: Observations of Sharp Oxalate Reductions in Stratocumulus Clouds at Variable Altitudes: Organic Acid and Metal Measurements During the 2011 E-PEACE Campaign, Environ. Sci. Technol., 47, 7747-7756, https://doi.org/10.1021/es4012383, 2013.

Sun. H., Sun, J., Zhu, C., Yu, L., Lou, Y., Li, R., and Lin, Z.: Chemical characterizations and sources of PM2.5 over the offshore Eastern China sea: Water soluble ions, stable isotopic compositions, and metal elements. Atmos. Pollut. Res., 13, 101410. https://doi.org/10.1016/j.apr.2022.101410, 2022.

Sun, M., Qi, Y., Li, W., Zhu, W., Yang, Y., Wu, G., Zhang, Y., Zhao, Y., Shi, J., Sheng, L., Wang, W., Liu, Y., Qu, W., Wang, X., and Zhou, Y. Investigation of a haze-to-dust and dust swing process at a coastal city in northern China part II: A study on the solubility of iron and manganese across aerosol sources and secondary processes. Atmos. Environ., 328, 120532. https://doi.org/10.1016/j.atmosenv.2024.120532, 2024.

Tang, W. Y., Llort, J., Weis, J., Perron, M. M. G., Basart, S., Li, Z. C., Sathyendranath, S., Jackson, T., Rodriguez, E. S., Proemse, B. C., Bowie, A. R., Schallenberg, C., Strutton, P. G., Matear, R., and Cassar, N.: Widespread phytoplankton blooms triggered by 2019-2020 Australian wildfires, Nature, 597, 370-375, https://doi.org/10.1038/s41586-021-03805-8, 2021.

Tian, H., Cheng, K., Wang, Y., Zhao, D., Lu, L., Jia, W., and Hao, J.: Temporal and spatial variation characteristics of atmospheric emissions of Cd, Cr, and Pb from coal in China, Atmos. Environ., 50, 157-163, https://doi.org/10.1016/j.atmosenv.2011.12.045, 2012.

Vu, T. V., Delgado-Saborit, J. M., and Harrison, R. M.: Review: Particle number size distributions from seven major sources and implications for source apportionment studies, Atmos. Environ., 122, 114-132, https://doi.org/10.1016/j.atmosenv.2015.09.027, 2015.

Wang, L., Qi, J. H., Shi, J. H., Chen, X. J., and Gao, H. W.: Source apportionment of particulate pollutants in the atmosphere over the Northern Yellow Sea, Atmos. Environ., 70, 425-434, https://doi.org/10.1016/j.atmosenv.2012.12.041, 2013.

Wang, Q., Qiao, L., Zhou, M., Zhu, S., Griffith, S., Li, L., and Yu, J. Z.: Source Apportionment of PM2.5 Using Hourly Measurements of Elemental Tracers and Major Constituents in an Urban Environment: Investigation of Time-Resolution Influence, J. Geophys. Res.-Atmos., 123, 5284-5300, https://doi.org/10.1029/2017JD027877, 2018.

Wang, W., Luo, C., Sheng, L., Zhao, C., Zhou, Y., and Chen, Y.: Effects of biomass burning on chlorophyll-a concentration and particulate organic carbon in the subarctic North Pacific Ocean based on satellite observations and WRF-Chem model simulations: A case study, Atmos. Res., 254, 105526, https://doi.org/doi.org/10.1016/j.atmosres.2021.105526, 2021.

https://doi.org/10.5194/egusphere-2025-4005
Preprint. Discussion started: 9 September 2025

Wang, W. C., He, Z. Z., Hai, S. F., Sheng, L. F., Han, Y. Q., and Zhou, Y.: Dust Aerosol's Deposition and its Effects on Chlorophyll-A Concentrations Based on Multi-Sensor Satellite Observations and Model Simulations: A Case Study, Front. Env. Sci.-Switz., 10, 875365, https://doi.org/10.3389/fenvs.2022.875365, 2022.

Wu, C., Huang, X. H. H., Ng, W. M., Griffith, S. M., and Yu, J. Z.: Inter-comparison of NIOSH and IMPROVE protocols for OC and EC determination: implications for inter-protocol data conversion, Atmos. Meas. Tech., 9, 4547-4560, https://doi.org/10.5194/amt-9-4547-2016, 2016.

Wu, R., Zhou, X., Wang, L., Wang, Z., Zhou, Y., Zhang, J., and Wang, W.: PM2.5 Characteristics in Qingdao and across Coastal Cities in China, Atmosphere, 8, https://doi.org/10.3390/atmos8040077, 2017.

Wu, S. P., Cai, M. J., Xu, C., Zhang, N., Zhou, J. B., Yan, J. P., Schwab, J. J., and Yuan, C. S.: Chemical nature of PM2.5 and PM10 in the coastal urban Xiamen, China: Insights into the impacts of shipping emissions and health risk, Atmos. Environ., 227, https://doi.org/10.1016/j.atmosenv.2020.117383, 2020.

Xu, B., Xu, H., Zhao, H., Gao, J., Liang, D., Li, Y., Wang, W., Feng, Y., and Shi, G.: Source apportionment of fine particulate matter at a megacity in China, using an improved regularization supervised PMF model. Sci. Total Environ., 879, 163198. https://doi.org/10.1016/j.scitotenv.2023.163198, 2023.

Xu, L., Liu, X. H., Gao, H. W., Yao, X. H., Zhang, D. Z., Bi, L., Liu, L., Zhang, J., Zhang, Y. X., Wang, Y. Y., Yuan, Q., and Li, W. J.: Long-range transport of anthropogenic air pollutants into the marine air: insight into fine particle transport and chloride depletion on sea salts. Atmos. Chem. Phys., 21, 17715-17726. https://doi.org/10.5194/acp-21-17715-2021, 2021.

Xu, L., Zhi, M. K., Liu, X. H., Gao, H. W., Yao, X. H., Yuan, Q., Fu, P. Q., and Li, W. J.: Direct evidence of pyrogenic aerosol iron by intrusions of continental polluted air into the Eastern China Seas, Atmos. Res., 292, 106839, https://doi.org/10.1016/j.atmosres.2023.106839, 2023.

Yang, F., Tan, J., Zhao, Q., Du, Z., He, K., Ma, Y., Duan, F., Chen, G., and Zhao, Q.: Characteristics of PM2.5 speciation in representative megacities and across China, Atmos. Chem. Phys., 11, 5207-5219, https://doi.org/10.5194/acp-11-5207-2011, 2011.

Yang, T., Chen, Y., Zhou, S., Li, H., Wang, F., and Zhu, Y.: Solubilities and deposition fluxes of atmospheric Fe and Cu over the Northwest Pacific and its marginal seas, Atmos. Environ., 239, 117763, https://doi.org/10.1016/j.atmosenv.2020.117763, 2020.

Yang, X., Zheng, M., Liu, Y., Yan, C., Liu, J., Liu, J., and Cheng, Y.: Exploring sources and health risks of metals in Beijing PM2.5: Insights from long-term online measurements. Sci. Total Environ., 814, 151954. https://doi.org/10.1016/j.scitotenv.2021.151954, 2022.

Yang, Y., Sun, M., Wu, G., Qi, Y., Zhu, W., Zhao, Y., Zhu, Y., Li, W., Zhang, Y., Wang, N., Sheng, L., Wang, W., Yu, X., Yu, J., Yao, X., and Zhou, Y.: Characteristics of aerosol aminiums over a coastal city in North China: Insights from the divergent impacts of marine and terrestrial influences. Sci. Total Environ., 918, 170672. https://doi.org/10.1016/j.scitotenv.2024.170672, 2024.

https://doi.org/10.5194/egusphere-2025-4005
Preprint. Discussion started: 9 September 2025

Yoon, J. E., Yoo, K. C., Macdonald, A. M., Yoon, H. I., Park, K. T., Yang, E. J., Kim, H. C., Lee, J. I., Lee, M. K., Jung, J., Park, J., Lee, J., Kim, S., Kim, S. S., Kim, K., and Kim, I.: Reviews and syntheses: Ocean iron fertilization experiments - past, present, and future looking to a future Korean Iron Fertilization Experiment in the Southern Ocean (KIFES) project, Biogeosciences, 15, 5847-5889, https://doi.org/10.5194/bg-15-5847-2018, 2018.

Yu, G., Zhang, Y., Yang, F., He, B., Zhang, C., Zou, Z., Yang, X., Li, N., and Chen, J.: Dynamic Ni/V Ratio in the Ship-Emitted Particles Driven by Multiphase Fuel Oil Regulations in Coastal China, Environ. Sci. Technol., 55, 15031-15039, https://doi.org/10.1021/acs.est.1c02612, 2021.

Yu, J. Z., Huang, X. F., Xu, J. H., and Hu, M.: When aerosol sulfate goes up, so does oxalate: Implication for the formation mechanisms of oxalate, Environ. Sci. Technol., 39, 128-133, https://doi.org/10.1021/es049559f, 2005.

Yuan, C. -S., Hung, C. -M., Hung, K. -N., Yang, Z. -M., Cheng, P. -H., and Soong, K. -Y.: Route-based chemical significance and source origin of marine PM2.5 at three remote islands in East Asia: Spatiotemporal variation and long-range transport. Atmos. Pollut. Res., 14, 101762. https://doi.org/10.1016/j.apr.2023.101762, 2023.

Zhang, G., Lin, Q., Peng, L., Yang, Y., Jiang, F., Liu, F., Song, W., Chen, D., Cai, Z., Bi, X., Miller, M., Tang, M., Huang, W., Wang, X., Peng, P. a., and Sheng, G.: Oxalate Formation Enhanced by Fe-Containing Particles and Environmental Implications, Environ. Sci. Technol., 53, 1269-1277, https://doi.org/10.1021/acs.est.8b05280, 2019.

Zhang, H., Li, R., Dong, S., Wang, F., Zhu, Y., Meng, H., Huang, C., Ren, Y., Wang, X., Hu, X., Li, T., Peng, C., Zhang, G., Xue, L., Wang, X., and Tang, M.: Abundance and Fractional Solubility of Aerosol Iron During Winter at a Coastal City in Northern China: Similarities and Contrasts Between Fine and Coarse Particles, J. Geophys. Res.-Atmos., 127, https://doi.org/10.1029/2021JD036070, 2022.

Zhang, J., Zhou, X., Wang, Z., Yang, L., Wang, J., and Wang, W.: Trace elements in PM2.5 in Shandong Province: Source identification and health risk assessment, Sci. Total. Environ., 621, 558-577, https://doi.org/10.1016/j.scitotenv.2017.11.292, 2018.

Zhang, Q., Jimenez, J. L., Canagaratna, M. R., Ulbrich, I. M., Ng, N. L., Worsnop, D. R., and Sun, Y.: Understanding atmospheric organic aerosols via factor analysis of aerosol mass spectrometry: a review, Anal. Bioanal. Chem., 401, 3045-3067, https://doi.org/10.1007/s00216-011-5355-y, 2011.

Zhang, T. L., Liu, J. Y., Xiang, Y. X., Liu, X. M., Zhang, J., Zhang, L., Ying, Q., Wang, Y. T., Wang, Y. N., Chen, S. L., Chai, F., and Zheng, M.: Quantifying anthropogenic emission of iron in marine aerosol in the Northwest Pacific with shipborne online measurements. Sci. Total Environ., 912, Article 169158. https://doi.org/10.1016/j.scitotenv.2023.169158, 2024.

Zhang, W., Peng, X., Bi, X., Cheng, Y., Liang, D., Wu, J., Tian, Y., Zhang, Y., and Feng, Y.: Source apportionment of PM2.5 using online and offline measurements of chemical components in Tianjin, China. Atmos. Environ., 244, 117942. https://doi.org/10.1016/j.atmosenv.2020.117942, 2021.

Zhang, Y., Cai, J., Wang, S., He, K., and Zheng, M.: Review of receptor-based source apportionment research of fine particulate matter and its challenges in China, Sci. Total. Environ., 586, 917-929, https://doi.org/10.1016/j.scitotenv.2017.02.071, 2017.

https://doi.org/10.5194/egusphere-2025-4005
Preprint. Discussion started: 9 September 2025

Zhang, Y., Deng, F., Man, H., Fu, M., Lv, Z., Xiao, Q., Jin, X., Liu, S., He, K., and Liu, H.: Compliance and port air quality features with respect to ship fuel switching regulation: a field observation campaign, SEISO-Bohai, Atmos. Chem. Phys., 19, 4899-4916, https://doi.org/10.5194/acp-19-4899-2019, 2019.

Zhang, Y., Schauer, J. J., Zhang, Y., Zeng, L., Wei, Y., Liu, Y., and Shao, M.: Characteristics of particulate carbon emissions from real-world Chinese coal combustion, Environ. Sci. Technol., 42, 5068-5073, https://doi.org/10.1021/es7022576, 2008.

Zhao, M., Zhang, Y., Ma, W., Fu, Q., Yang, X., Li, C., Zhou, B., Yu, Q., and Chen, L.: Characteristics and ship traffic source identification of air pollutants in China's largest port, Atmos. Environ., 64, 277-286, https://doi.org/10.1016/j.atmosenv.2012.10.007, 2013.

Zhao, R., Han, B., Lu, B., Zhang, N., Zhu, L., and Bai, Z.: Element composition and source apportionment of atmospheric aerosols over the China Sea. Atmos. Pollut. Res., 6, 191-201. http://doi.org/10.5094/APR.2015.023, 2015.

Zhou, Y., Huang, X. H., Bian, Q., Griffith, S. M., Louie, P. K. K., and Yu, J. Z.: Sources and atmospheric processes impacting oxalate at a suburban coastal site in Hong Kong: Insights inferred from 1year hourly measurements, J. Geophys. Res.-Atmos., 120, 9772-9788, https://doi.org/10.1002/2015JD023531, 2015.

Zhou, Y.: Elevated Anthropogenic Contributions to Trace Elements in Marine Aerosols Compared to Coastal Qingdao in Eastern China. Figshiare [Dataset]. https://doi.org/10.6084/m9.figshare.29625746, 2025.

Zhu, W., Qi, Y., Tao, H., Zhang, H., Li, W., Qu, W., Shi, J., Liu, Y., Sheng, L., Wang, W., Wu, G., Zhao, Y., Zhang, Y., Yao, X., Wang, X., Yi, L., Ma, Y., and Zhou, Y.: Investigation of a haze-to-dust and dust swing process at a coastal city in northern China part I: Chemical composition and contributions of anthropogenic and natural sources, Sci. Total. Environ., 851, 158270, https://doi.org/10.1016/j.scitotenv.2022.158270, 2022.

Zhu, Y., Li, W., Wang, Y., Zhang, J., Liu, L., Xu, L., Xu, J., Shi, J., Shao, L., Fu, P., Zhang, D., and Shi, Z.: Sources and processes of iron aerosols in a megacity in Eastern China, Atmos. Chem. Phys., 22, 2191-2202. https://doi.org/10.5194/acp-22-2191-2022, 2022.

Zhuang, G., Yi, Z., Duce, R. A., and Brown, P. R.: Link between iron and sulphur cycles suggested by detection of Fe(n) in remote marine aerosols. Nature, 355, 537-539. https://doi.org/10.1038/355537a0, 1992